The 2023 World Congress on
Advances in Structural Engineering and Mechanics (ASEM23)
GECE, Seoul, Korea, August 16-18, 2023

Nonlinear static progressive collapse analysis for RC building frames subjected to initial lateral story drift

Meng-Hao Tsai[1)]

[1)] *Department of Civil Engineering, National Pingtung University of Science and Technology, Pingtung County 912, Taiwan*
[1)] mhtsai@mail.npust.edu.tw

ABSTRACT

Many studies were conducted to investigate the progressive collapse resistance of RC building frames under column loss without story drift. This study intends to investigate the effect of possible initial story drift on the progressive collapse resistance of seven seismically designed RC building frames. Nonlinear static analyses were conducted to obtain the load-deflection responses under column-loss and initial story drift conditions. The analysis results show that increasing the initial story drift led to a decrease in the collapse resistance and the corresponding chord rotation. When the initial story drift was increased to 1.5%, lateral-sway failure mode was likely to occur under the column-loss conditions. The collapse resistance reduction varied with the initial story drift approximately in a linear relation. Approximately, 20% reduction in the collapse resistance was observed with an initial story drift of 1.5%.

1. INTRODUCTION

The first priority of structural design is to ensure that the designed structures have sufficient strengths during their life cycles under all possible loadings. The loadings may be environmental, such as earthquake and wind, or man-made, such as explosion and vehicle collision. The structural design may be dominated by different loadings, depending on the environmental conditions that the structure is dealt with. Since the collapse of the World Trade Center during the terrorist attacks in 2001 (Bazant and Zhou 2002; Newland and Cebon 2002), vulnerability to progressive collapse has become a significant issue in structural safety. To deal with this low-probability high-consequence events, the US General Service Administration (GSA) and Department of Defense (DoD) announced their first issue of design guidelines for buildings to resist progressive collapse in 2003 (GSA 2003) and 2005 (DoD 2005), respectively. Structural redundancy was addressed and four typical column-loss conditions were recommended to evaluate the progressive collapse potentials in the GSA guidelines. Tie forces and alternate load path (ALP) methods were suggested as the design

---

[1)] Professor

strategies in the DoD guidelines. Since then, the ALP analysis under different postulated column-loss conditions has been considered as a fundamental method to assess the progressive collapse resistance of building frames. Tsai and Lin (2008) conducted ALP analysis with linear static, nonlinear static, and nonlinear dynamic methods to investigate the collapse resistance of a seismically designed reinforced concrete (RC) building frame. Izzuddin *et al*. (2008) proposed a simplified procedure for progressive collapse assessment of building frames using ALP analysis method. Khandelwal and El-Tawil (2011) suggested the pushdown analysis technique can be used to estimate the residual capacity and failure mode of damaged frames. The idea was in fact identical to the ALP method. Similarly, Xu and Ellingwood (2011) used the nonlinear static pushdown technique to evaluate the vulnerability of three steel frames under column loss. Fallon *et al*. (2016) recommended that uniform pushdown approach was more suitable for quantifying structural robustness of building frames.

The column-loss scenario was often achieved by artificially removing the designated member before performing the nonlinear analyses. Although localized accidental loadings such as explosion or vehicle impact were assumed for the cause of column loss, some studies were involved with the progressive collapse behavior of building frames under lateral seismic loadings. Beham *et al*. (2019) used a ten-story steel moment resisting frame to investigate the progressive collapse vulnerability under beam-removal scenarios after horizontal earthquake excitations. They concluded that upper stories were more vulnerable to progressive collapse failure than lower stories. Elshaer *et al*. (2017) conducted three-dimensional nonlinear dynamic analyses for an RC structure subjected to column loss under seismic excitations. The study indicated that losing a column during a seismic action could be more critical than that under gravitational load only. Tavakoli and Hasani (2017) conducted nonlinear time-history analyses for a five-story steel special moment frame to study the seismic progressive collapse behavior under earthquakes with different characteristics. They revealed that the progressive collapse potential is dependent on the location of the removed column and the number of stories. Tavakoli and Afrapoli (2018) investigated the progressive collapse scenarios of steel frames having various lateral load resisting systems under seismic excitations. Better progressive collapse performances were observed for braced steel frames.

It was observed from literature review that most studies concerned with the progressive collapse resistances either under the gravitational loadings or the lateral seismic loadings. Under lateral seismic loads, the building frames may lose the supporting column at first and then collapse under gravitational loadings. Therefore, this numerical study intended to investigate the effect of lateral story drift on the gravitational progressive collapse resistance for RC building frames. The analysis methods were explained and applied to seven seismically designed RC building frames. Nonlinear static pushover and pushdown analyses were conducted to examine the effect of various story drifts on the progressive collapse resistance under bottom column-loss conditions.

2. COLUMN REMOVAL PROCEDURE

The static equilibrium equation of a building frame subjected to gravitational and lateral loadings may be written as

$$[K_0]\{y_0\} = \{P\} + \{W\} \quad (1)$$

where $[K_0]$ is the structural stiffness matrix, $\{y_0\}$ is the nodal displacement, {*P*} is and lateral loading, and {*W*} is the gravitational loading. Assume that the stiffness matrix of the removed column is expressed as $[k_0]$. Then, the above equation can be rewritten as

$$[K_1]\{y_0\} + [k_0]\{y_0\} = \{P\} + \{W\} \quad (2)$$

where $[K_1]$ is the structural stiffness matrix of the remaining structure. In Eq. (2), the second term of the left-hand side can be replaced with the internal force, $\{p_0\}$, of the removed column and moved to the right-hand side. Thus, Eq.(2) is rewritten as

$$[K_1]\{y_0\} = \{P\} + \{W\} - \{p_0\} \quad (3)$$

Both Eq.(1) and Eq.(2) represent the intact structure under the lateral and gravitational loadings. The term $\{p_0\}$ in Eq.(3) should be removed to obtain the static equilibrium under column loss. If $\{p_0\}$ was added to both sides of Eq.(3), certain structural response would be induced to the remaining structure. If the induced static structural response was expressed as $[K_1]\{\delta_0\} = \{p_0\}$, then the equilibrium equation after column removal would be written as

$$[K_1]\{y_0\} + [K_1]\{\delta_0\} = \{P\} + \{W\} \quad (4)$$

where $\{\delta_0\}$ is the structural displacement induced by the internal force of the removed column. It could be expressed as

$$[K_1]\{y_1\} = \{P\} + \{W\} \quad (5)$$

where $\{y_1\} = \{y_0\} + \{\delta_0\}$ was the total structural displacement after column removal.

From the above derivation, it was known that irrespective of the column removal and loading procedure, the structural frame should present the same displacement response $\{y_1\}$ if it was elastic under the column-loss condition. However, the displacement response could be different if it was inelastic after the column removal. Hence, two nonlinear static pushdown analysis procedures for the column-loss frames were considered in this study and described as follows.

<u>Method (A)</u> Remove the postulated column from the structural model to result in the $[K_1]$structural stiffness. Apply the lateral loading *{P}* to the column-removed model to a specified bottom story drift θ. At last, apply the gravitational loading *{W}* and conduct

nonlinear static pushdown analysis for the peak collapse resistance. This procedure implies that the structural response is directly solved from Eq.(5) without considering the internal forces of the removed column, as graphically demonstrated in Fig. 1.

Method (B) Conduct pushover analysis under the lateral load pattern *{P}* to the specified bottom story drift θ. Remove the postulated column and release the internal force $\{p_0\}$. Conduct pushdown analysis under the load pattern *{W}* until the collapse load of the column-loss model. The procedure is graphically demonstrated in Fig. 2. This method considers the effect of the internal force $\{p_0\}$, which is neglected in Method (A). From a previous study (Tsai 2012), it was shown that Methods (A) and (B) would have the same results for elastic column-removed response.

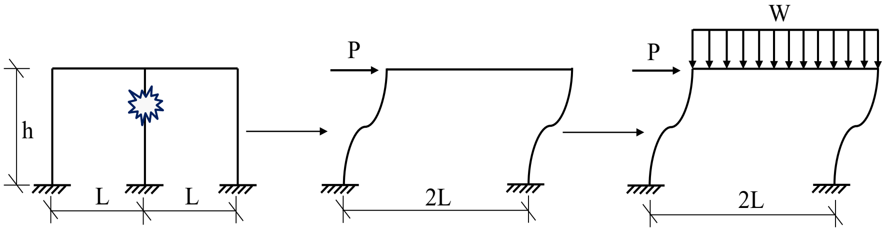

Fig. 1 Illustration of Method (A) analysis procedure

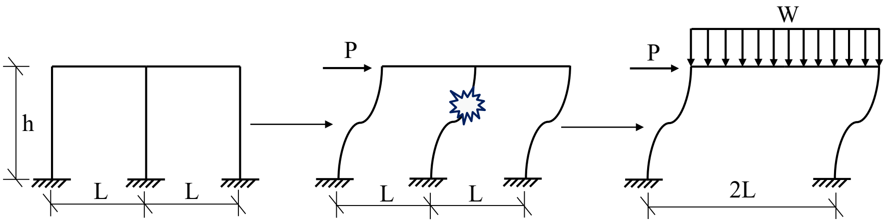

Fig. 2 Illustration of Method (B) analysis procedure

In this study, nonlinear static analyses were conducted for seven seismically designed RC building frames to demonstrate the effects of the lateral story drift on the progressive collapse resistance under column loss. The influences of seismic demand, span length, and number of stories on the collapse resistance were also investigated.

3. DESIGN AND MODELING OF THE RC BUILDING FRAMES

Considering the variation of seismic demand, story number, and span length, seven RC moment-resisting building frames with a constant story height of 3 m were designed based on the Seismic Design Specifications and Commentary for Buildings of Taiwan (MOI 2005). The compressive strength of concrete and tensile yield strength of reinforcement were assumed as 27.5 MPa (280 kgf/cm^2) and 412 MPa (4200 kgf/cm^2), respectively. As shown in Fig. 3, each building frame had a regular four bay-by-three bay plan layout. The design dead load (DL) was composed of the frame weight, a uniform slab loading of 3.92 kN/m^2 (400 kgf/m^2) and the weight of 24 cm-thick exterior non-structural brick walls. The service live load (LL) is 1.73 kN/m^2 (300 kgf/m^2).

Considering the typical low, medium, and high seismic demands in Taiwan, three seismic coefficients, C_s = 0.10, 0.15, and 0.22 were determined, respectively. Three five-story frames with a span length of 4, 6, and 10 m, respectively, were designed with a constant C_s of 0.15. Three ten-story frames with C_s of 0.10, 0.15, and 0.22, respectively, were designed with a constant span length of 6 m. A fifteen-story frame was designed with a span length of 6 m and C_s of 0.15. The equivalent lateral seismic design load was story-wise distributed in an inversely triangular variation form. The effective structural weight was equal to the sum of the design dead load (DL) and a quarter of live load (LL). Load combinations of (1.2DL+1.6LL) and (1.2DL+1.0LL+1.0EQ) were considered for the structural design. The column sections were determined according to the strong column-and-weak beam mechanism (ACI 2011). The design results and designations of the seven building frames are summarized in Table 1. For convenience, they were designated by their number of stories, span lengths, and seismic coefficients. For example, the designation of 05S06R15 stands for the five-story building frame with span length of 6 m and seismic coefficient of 0.15.

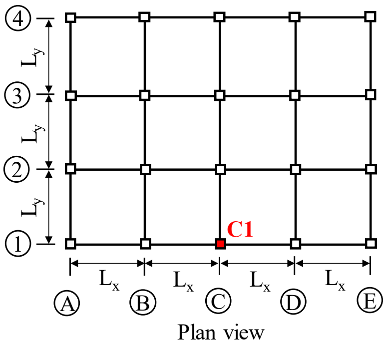

Fig. 3 Plan view of the example building frames

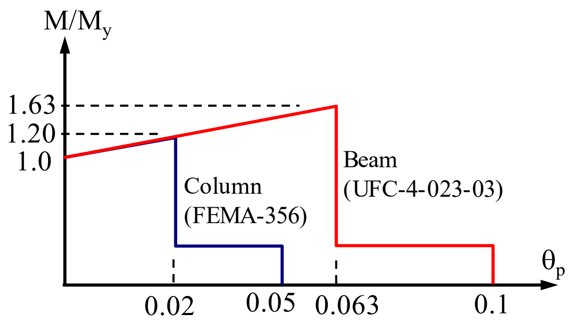

Fig. 4 Flexural hinge properties used in the analysis

Table 1 Detailed design results and designations of the seven example buildings

Designation	Story	Beam section (cm^2)	Beam reinforcement Top (ρ)	Beam reinforcement Bottom (ρ)	Column section (cm^2)	Column reinforcement
05S04R15	1~3F 4~5F	50×35	5#6 (0.9%) 3#6 (0.6%)	3#6 (0.6%) 2#6 (0.4%)	55×55	16-#6 (1.5%)
05S06R15	1~3F 4~5F	60×45	6#7 (1.0%) 4#7 (0.6%)	3#7 (0.5%) 3#7 (0.5%)	65×65	16-#7 (1.5%)
05S10R15	1~3F 4~5F	80×60	12#7(0.6%) 10#7(0.5%)	7#7(0.6%) 7#7(0.6%)	90×90	24-#9 (1.9%)
10S06R10	1~4F 5~7F 8~10F	70×50	8#7 (0.9%) 7#7 (0.8%) 5#7 (0.6%)	5#7 (0.6%) 4#7 (0.5%) 3#7 (0.4%)	75×75	24-#7 (1.7%)
10S06R15	1~4F 5~7F 8~10F	80×60	9#8 (1.0%) 8#8 (0.9%) 5#8 (0.6%)	6#8 (0.7%) 5#8 (0.6%) 3#8 (0.3%)	85×85	24-#8 (1.7%)
10S06R22	1~4F 5~7F 8~10F	85×65	10#9 (1.2%) 9#9 (1.0%) 7#9 (0.8%)	8#9 (0.9%) 7#9 (0.8%) 5#9 (0.6%)	90×90	24-#9 (1.9%)

15S06R15	1~5F 5~10F 10~15F	90×70	10#9 (1.1%) 9#9 (0.9%) 6#9 (0.7%)	8#9 (0.9%) 8#9 (0.9%) 5#9 (0.5%)	95×95	28-#9 (2%)

Beam-column structural models were constructed by using the SAP2000 (2021) commercial program. As shown in Fig. 4, flexural hinge properties recommended by the DoD (2016) and the FEMA-356 (FEMA 2000) guidelines were assumed for the plastic hinges assigned to the beam ends and column ends, respectively. A post-yield stiffness ratio of 5% was used for the plastic hinges. Table 2 shows the fundamental periods in their longitudinal and transverse directions. It is observed from the table that the ten- and fifteen-story building frames were a little stiffer than conventional design. This was caused by that for each building frame, the section depths of beam members were held constant for simplicity. Nevertheless, the structural models were appropriate for investigating the effect of the initial story drift on the progressive collapse resistance of the building frames.

Table 2 Fundamental periods, yield base shears, and seismic coefficients of the building frames

Building	Transverse			Longitudinal		
	Period (s)	Vy (kN)	Cs	Period (s)	Vy (kN)	Cs
05S04R15	0.536	1781	0.140	0.523	1878	0.148
05S06R15	0.590	3107	0.127	0.576	3263	0.134
05S10R15	0.610	11980	0.164	0.595	12663	0.173
10S06R10	0.988	4954	0.090	0.958	5299	0.096
10S06R15	0.812	9254	0.147	0.786	9941	0.158
10S06R22	0.747	16504	0.245	0.723	17469	0.260
15S06R15	1.094	17122	0.158	1.045	18165	0.167

4. NUMERICAL ANALYSIS RESULTS

4.1 Normalized pushdown load-deflection response

Nonlinear static analyses were conducted as described in Methods (A) and (B). In addition to the case of zero drift, six specified bottom story drift ratios were 0.3%, 0.5%, 0.8%, 1%, 1.2%, and 1.5%. The middle column in the longitudinal side of the building frames, which was indicated as C1 in Fig. 3, was selected as the removed column. In Method (A), the column C1 was removed and pushover analysis was then conducted using the equivalent lateral load pattern until the specified bottom story drift was reached. Under the sustaining lateral deformation, nonlinear static pushdown analysis under uniformly distributed loadings was performed to obtain the peak collapse resistance.

Fig. 6(a)~6(g) show the normalized pushdown load-deflection curves of the seven building frames under the specified story drift ratios. In the figures, the ordinate was obtained from dividing the pushdown loading by the structural effective seismic weight. The abscissa was the chord rotation, which was obtained from dividing the vertical deflection of the column-removed joint by the span. All curves started from the initial condition of sustaining self-weight. It is observed from the figures that the peak collapse resistance and corresponding chord rotation decreased with increasing the story drift. The lateral story drift did not change the plastic stiffness when full-plastic mechanism was activated. However, a larger lateral story drift may reduce the elastoplastic stiffness before the activation of full-plastic mechanism, especially for the five-story building cases, as observed from Fig. 6(a)~6(c).

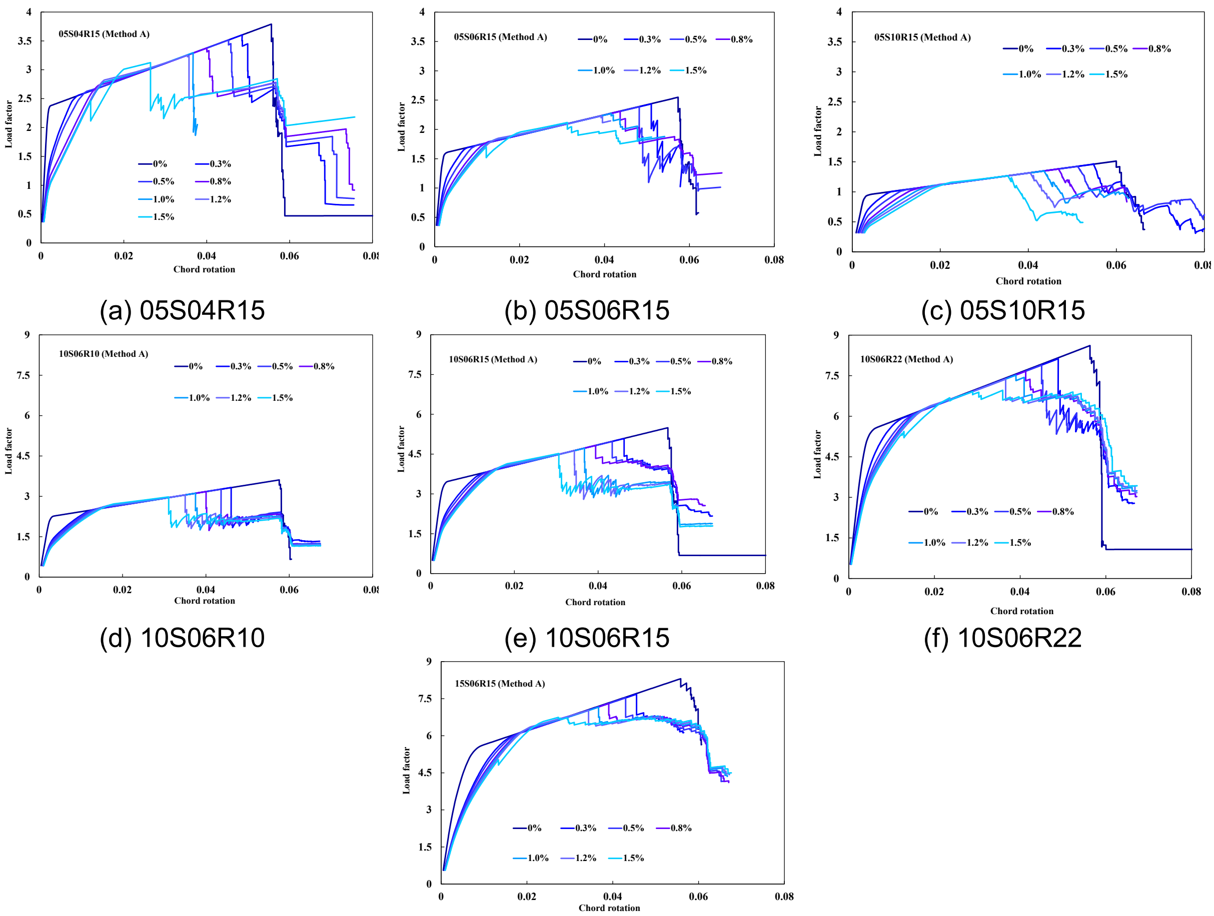

(a) 05S04R15 (b) 05S06R15 (c) 05S10R15

(d) 10S06R10 (e) 10S06R15 (f) 10S06R22

(g) 15S06R15

Fig. 6 Normalized pushdown load-deflection curves from Method (A)

In Method (B), pushover analysis was conducted for the intact building frames to the specified story drift at first. The column C1 was removed and the internal section forces of the column joint with the two-span beams were counteracted by imposing equal-but-opposite forces. After that, nonlinear static pushdown analysis was conducted. Fig. 7(a)~7(g) show the normalized pushdown load-deflection curves of the seven building frames under the specified story drift ratios. Similar to the results of Method (A), the peak collapse resistance and corresponding chord rotation decreased with increasing the story drift. It was observed from the comparison of the five-story cases that Method (B) resulted in moderately lower peak resistances than Method (A) when the story drift ratio was larger than 1.2%. This was caused by the release of the internal section forces of the removed column, which exacerbated the plastic hinges induced by the lateral deformation. However, the effect of the internal section forces on the load-deflection response was less significant for the ten- and fifteen-story building cases. In general, Methods (A) and (B) had similar load-deflection responses when the imposed story drift ratio was less than 1%.

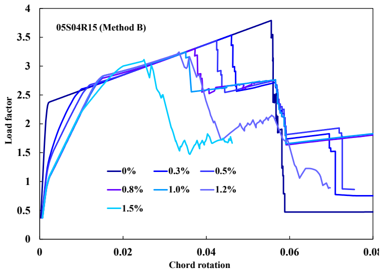

(a) 05S04R15

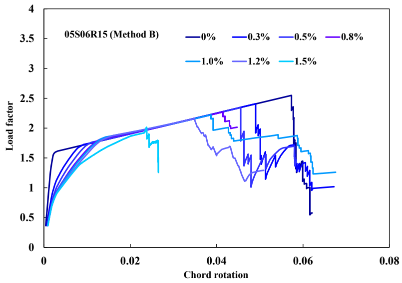

(b) 05S06R15

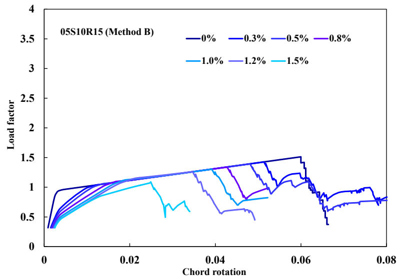

(c) 05S10R15

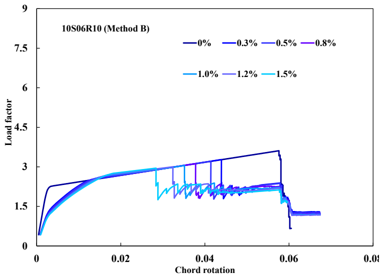

(d) 10S06R10

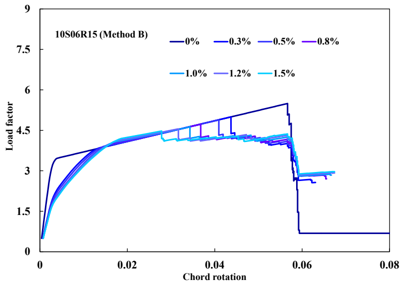

(e) 10S06R15

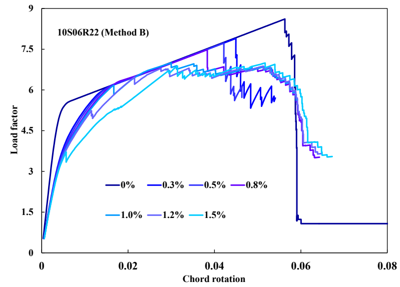

(f) 10S06R22

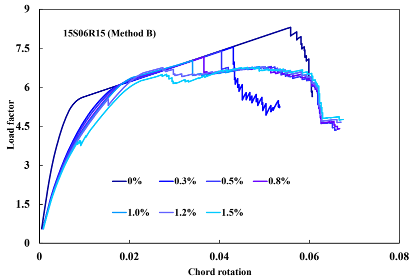

(g) 15S06R15

Fig. 7 Normalized pushdown load-deflection curves from Method (B)

4.2 Story drift-chord rotation curves

Due to the initial story drift, the imposed vertical downward loading on the column-removed building frames would induce secondary moment to the column ends and increase the structural lateral deformation. Plastic hinges may be generated at the column ends because of the increased moments and lateral deformation. This could further provoke lateral-sway failure mechanism for the building frames.

Fig. 8(a)~8(g) show the variation of the bottom story drift with the chord rotation of the two-span beams obtained from Method (A). It was observed from the figures that at the beginning of the downward loading, the chord rotation increased proportionally with the story drift. However, in most cases, the column-removed building frames were dominated by the downward deflection mode when the chord rotation exceeded 0.015 and the increase of story drift was suspended. This downward-dominated region was corresponding to the plastic region of significant yielding up to the collapse resistance, as shown in Fig. 6. The lateral deflection was resumed after the collapse resistance and failure mechanism was generated thereafter. Furthermore, when the initial story drift was increased, the downward-dominated mode could occur at a larger and terminate at a smaller chord rotation, as observed from Fig. 8(d) and 8(e). When the initial story drift was increased to 1.5%, as shown in Fig. 8(c), 8(f), and 8(g), both the chord rotation and the story drift could proportionally increase until the collapse resistance. Therefore, the downward-dominated region was not triggered and a lateral-sway failure mode was induced instead.

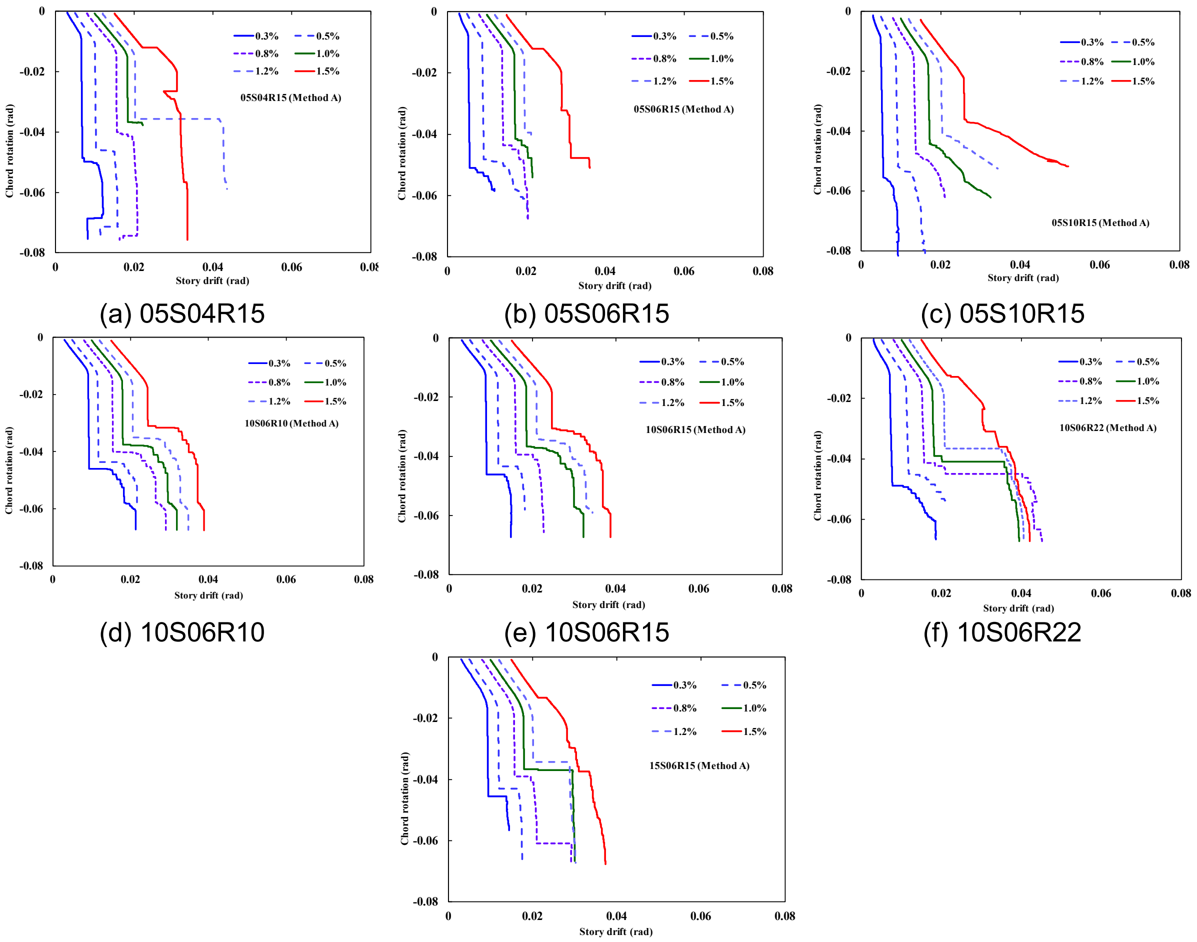

(a) 05S04R15 (b) 05S06R15 (c) 05S10R15

(d) 10S06R10 (e) 10S06R15 (f) 10S06R22

(g) 15S06R15

Fig. 8 Story drift and chord rotation curves from Method (A)

Fig. 9(a)~9(g) show the variation of the bottom story drift with the chord rotation of the two-span beams obtained from Method (B), which exhibited similar behavior with that from Method (A). However, it was observed that the variation of the response curves changed from downward-dominated deformation to lateral-sway deformation in some cases. These cases included the 1.2% and 1.5% story drift responses of 05S04R15, 1.5% story drift response of 05S06R15 and 05S10R15, 1.0% and 1.2% story drift response of 10S06R22, and 1.2% story drift response of 15S06R15. It was known that with the initial story drift before column removal, the two-span beams were subjected to two pairs of positive and negative moments on each side of the removed column. When the joint internal force was released, flexural demand was increased for one pair of the moments but decreased for the other. This could increase the plastic hinge rotation demands on the pair with increased moments and exacerbate the lateral sway mechanism.

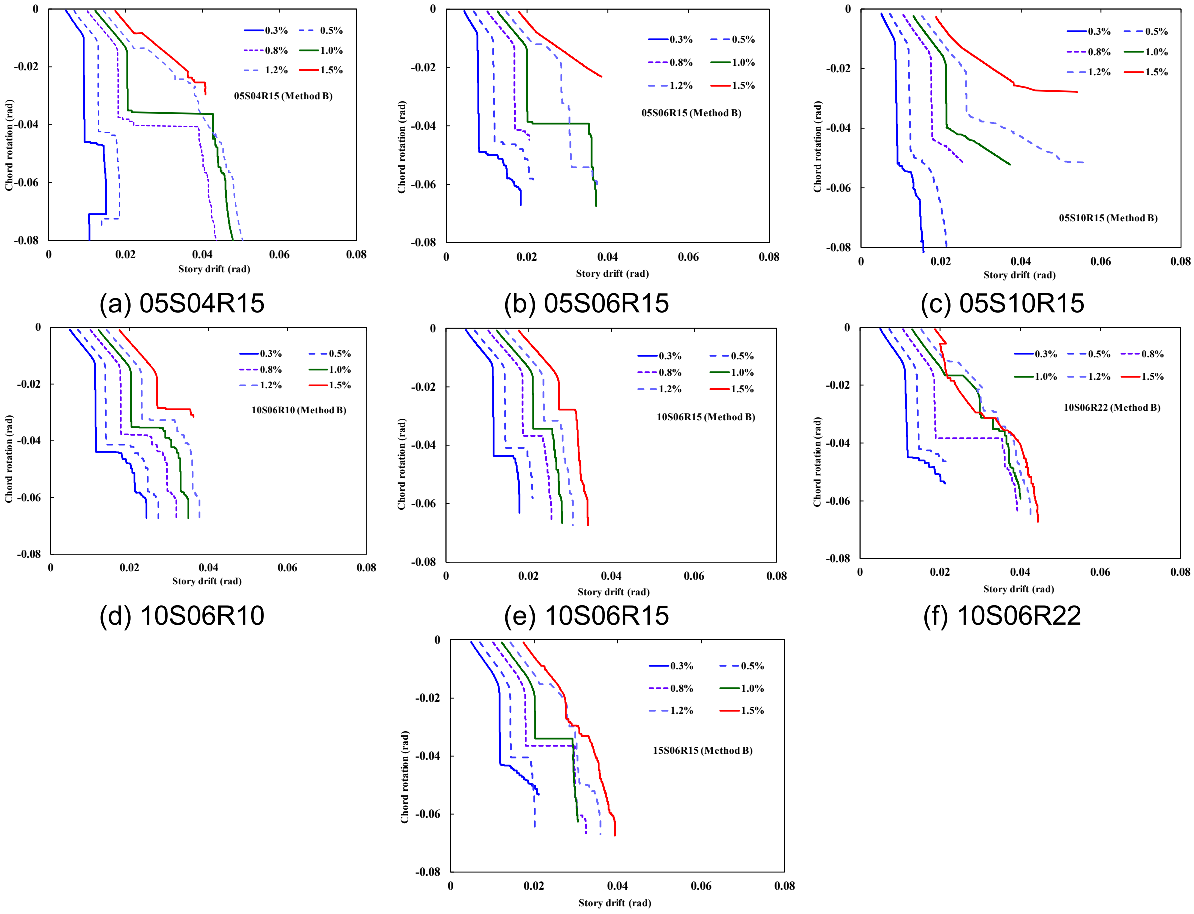

(a) 05S04R15 (b) 05S06R15 (c) 05S10R15

(d) 10S06R10 (e) 10S06R15 (f) 10S06R22

(g) 15S06R15

Fig. 9 Story drift and chord rotation curves from Method (B)

From the observation of the analysis results, it was realized that the initial lateral story drift may reduce the collapse resistance and activate the sway failure mechanism, which could induce overturn collapse for the building. When the story drift was less than 1%, the structural failure was induced by the downward-dominated progressive collapse. In such case, the plastic hinges of the bay members over the removed column were subjected to more serious damage than the bottom columns, as shown in Fig. 10 (a). However, when the initial story drift was increased, both the vertical and lateral deflections were monotonically increased under the gravitational loading. The damage to the plastic hinges of the bottom columns could be comparable with that of the bay members over the removed column, as shown in Fig. 10(b). Therefore, the building was prone to lateral-sway collapse.

4.3 Effect of story drift on the strength reduction ratio

From the load-deflection response presented in Section 4.1, it was realized that the collapse resistance was decreased with increased story drift ratio. To quantify the effect of the story drift ratio on the collapse resistance, the collapse resistances of the building frames with initial story drift were divided by that without. The resistance ratios were shown in Fig. 11(a) for the five-story frames and in Fig. 11(b) for the others. It is observed that most cases appeared to have approximately consistent resistance reduction with the increased story drift, with slightly more reduction for Method (B). The collapse resistance under an initial story drift of 1.5% was approximately reduced to 80% of that without story drift. Strength reduction of the 05S10R15 case was more significant than others and the consideration of the internal section force had apparently adverse effect on the strength when the story drift ratio was larger than 1%. It should be mentioned that design of the 05S10R15 case was controlled by the gravitational load combination. Therefore, special care should be given for the effect of lateral story drift on the collapse resistance of long span frames.

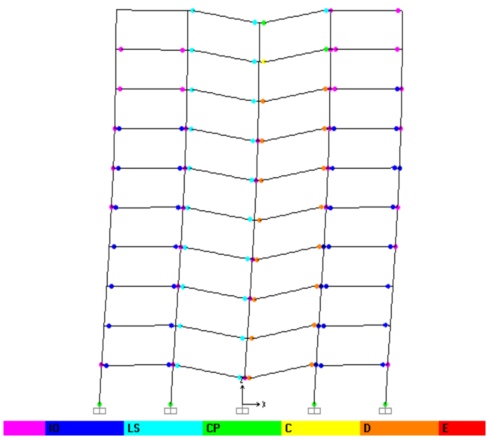

Fig. 10(a) Status of plastic hinge damage for Case 10S06R22 under 0.5% story drift with Method (A)

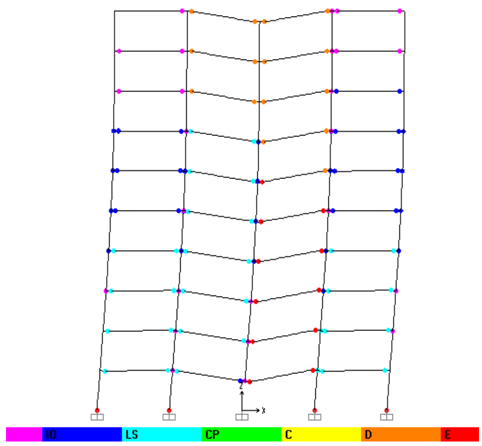

Fig. 10(b) Status of plastic hinge damage for Case 10S06R22 under 1.5% story drift with Method (A)

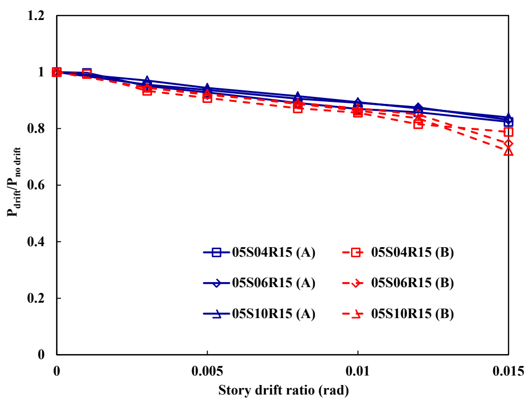

Fig. 11(a) Effect of story drift on the resistance ratio for the five-story frames

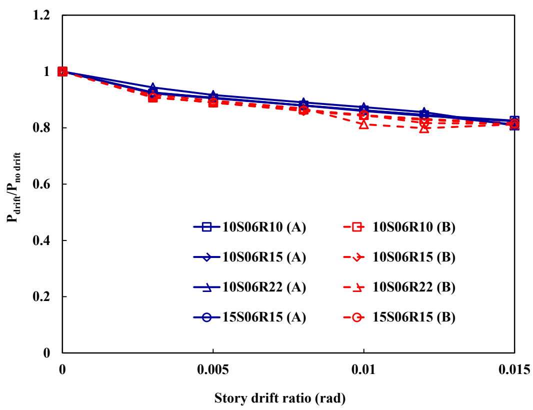

Fig. 11(b) Effect of story drift on the resistance ratio for the ten- and fifteen-story frames

5. CONCLUSIONS

This study investigated the effect of lateral story drift on the progressive collapse resistance of RC building frames under column loss using nonlinear static (NS) analysis approach. Two analysis methods were adopted in the NS analysis. The postulated bottom column was removed before the NS pushover stage in Method (A), while it was removed after the NS pushover stage in Method (B). In both methods, NS pushdown analyses were conducted for the RC building frames under column loss after imposing an initial bottom story drift. Analysis results indicated that increasing the story drift led to a reduction in the collapse resistance and the corresponding chord rotation. Both methods could have similar NS pushdown response to the peak resistance. However, Method (B) was more vulnerable to lateral-sway failure mode under larger story drift demand. This could lead to a lower collapse resistance with a larger chord rotation demand. The resistance ratio of the RC building frames with initial story drift to that without was approximately linearly decreased with increasing story drift. The resistance ratio was approximated to 80% with an initial story drift of 1.5%.

ACKNOWLEDGEMENT

The financial support of this study was provided by the National Science and Technology Council, Taiwan, under the Grant No. MOST 108-2221-E-020-002-MY2.

REFERENCES

ACI (2011), *Building code requirements for structural concrete and commentary*, American Concrete Institute (ACI), Farmington Hills, MI.

Bazant, Z.P., and Zhou, Y. (2002). “Why did the World Trade Center collapse?- simple analysis,” *Journal of Engineering Mechanics*, **128**(1), 2-6.

Beham, B., Shojaei, F., Ronagh, H.R. (2019), “Seismic progressive-failure analysis of tall steel structures under beam-removal scenarios,” *Frontiers of Structural and Civil Engineering*, **13**(4): 904–917.

DoD (2005), *Design of buildings to resist progressive collapse*, Unified Facilities Criteria UFC-4-023-03, Department of Defense (DoD), USA.

DoD (2016), *Design of buildings to resist progressive collapse*, Unified Facilities Criteria UFC-4-023-03, Department of Defense (DoD), USA.

Elshaer, A., Mostafa, H., and Salem, H. (2017), “Progressive collapse assessment of multistory reinforced concrete structures subjected to seismic actions. *KSCE Journal of Civil Engineering*, **21**(1), 184-194.

Fallon, C.T., Quiel, S.E., and Naito, C.J. (2016), “Uniform pushdown approach for quantifying building-frame robustness and the consequence of disproportionate collapse,” *Journal of Performance of Constructed Facilities*, **30**(6), 04016060-1-12.

FEMA (2000), *Prestandard and Commentary for the Seismic Rehabilitation of Buildings*, FEMA-356. Federal Emergency Management Agency (FEMA), Washington, D.C.

GSA (2003), *Alternate Path Analysis & Design Guidelines for Progressive Collapse Resistance*, The U.S. General Service Administrations (GSA), Washington D.C.

Izzuddin B.A., Vlassis A.G., Elghazouli A.Y., and Nethercot D.A. (2008). "Progressive collapse of multi-storey buildings due to sudden column loss-Part I: Simplified assessment framework," *Engineering Structures*, **30**(5), 1308–1318.

Khandelwal, K. and El-Tawil, S. (2011), "Pushdown resistance as a measure of robustness in progressive collapse analysis," *Engineering Structures*, **33**(9), 2653–2661.

MOI (2005), *Seismic Design Specifications and Commentary for Buildings of Taiwan*, Construction and Planning Agency, Ministry of the Interior (MOI), Taiwan.

Newland, D.E. and Cebon, D. (2002). "Could the World Trade Center have been modified to prevent its collapse?" *Journal of Engineering Mechanics*, **128**(7), 795-800.

SAP2000 (2021), *Linear and nonlinear static and dynamic analysis and design of three-dimensional structures*, Computers and Structures Inc., Berkeley, CA.

Tavakoli, H.R. and Hasani, A.H. (2017), "Effect of earthquake characteristics on seismic progressive collapse potential in steel moment resisting frame," *Earthquakes and Structures*, **12**(5): 529-541.

Tavakoli, H.R., Afrapoli, M.M. (2018), "Robustness analysis of steel structures with various lateral load resisting systems under the seismic progressive collapse," *Engineering Failure Analysis*, **83**, 88–101.

Tsai, M.H. and Lin, B.H. (2008), "Investigation of progressive collapse resistance and inelastic response for an earthquake-resistant RC building subjected to column failure," *Engineering Structures*, **30**(12), 3619-3628.

Tsai, M.H. (2012), "Evaluation of different loading simulation approaches for progressive collapse analysis of regular building frames," *Structure and Infrastructure Engineering*, **8**(8), 765-779.

Xu, G. and Ellingwood, B.R. (2011), "An energy-based partial pushdown analysis procedure for assessment of disproportionate collapse potential," *Journal of Constructional Steel Research*, **67**(3), 547–555.